SRF PHOTOINJECTOR TESTS AT HOBICAT*

A. Neumann†, W. Anders, R. Barday, A. Jankowiak, T. Kamps, J. Knobloch,
O. Kugeler, A. Matveenko, T. Quast, J. Rudolph, S. Schubert, J. Voelker
Helmholtz-Zentrum-Berlin, 12489 Berlin, Germany
J. Smedley, Brookhaven National Laboratory, Upton, NY, USA
J. Sekutowicz, DESY, 22607 Hamburg, Germany
P. Kneisel, Jefferson Laboratory, Newport News, VA, USA
R. Nietubyc, A. Soltan Institute, Swierk, Poland
I. Will, Max-Born Institute, 12489 Berlin, Germany
G. Lorenz, Fritz-Haber-Institut der Max-Planck-Gesellschaft, 14195 Berlin, Germany

Abstract

In collaboration with Jefferson Laboratory, DESY and the A. Soltan Institute HZB developed a fully superconducting RF photo-injector as a first step towards a high average current electron source for the B*ERL*inPro ERL. This setup consists of a 1.6 cell superconducting gun cavity with a lead cathode plasma-arc deposited on the half cell backwall and a superconducting solenoid. The system, including a warm diagnostic beam-line section, was recently installed in the HoBiCaT test facility to study beam dynamics within the ERL parameter range. This paper will give an overview of the horizontal cavity tests, dark current studies and beam measurements.

INTRODUCTION

In the framework of the B*ERL*inPro Energy Recovery Linac project [1] HZB needs to develop a high current CW photoinjector delivering an average beam current of 100 mA at a normalized emittance of 1mm mrad and an exit kinetic energy above 1.5 MeV. This implies the usage of a high quantum efficiency normal-conducting cathodes at highest launch fields possible and a laser repetition rate of 1.3 GHz, filling every RF bucket, such that a CW operated SC photoinjector cavity is mandatory to achieve the required voltage. Thus also a damping of unwanted higher order modes has to be studied and a design has to be found which allows maximum field at strong beam-loading given the RF power constraints of the fundamental couplers. To achieve these challenging goals HZB will follow a three stage approach [2, 3]. The first step is a fully superconducting system of a 1.6 cell cavity, a superconducting lead photocathode and a superconducting solenoid for beam dynamics studies. It is being developed in a collaboration with DESY, Jefferson Laboratory and the A. Soltan Institute. This photoinjector will be used to demonstrate the short-pulse beam dynamics using a SC solenoid in the ERL parameter range. The following two injector systems will feature the insert of a normal conducting cathode including a choke filter system and finally a HOM damping scheme to handle the high average current.

This paper will give a first overview about the horizontal cavity tests, dark current studies and beam measurements.

Table 1: Cavity electromagnetic design parameters

Frequency π-mode	1300 MHz
Frequency 0-mode	1281 MHz
E_{peak}/E_{cath}	1.0
E_{peak}/E_{acc} (β=1)	1.86
H_{peak}/E_{acc}	4.4 mT/(MV/m)
Geometry factor	212 Ω
R/Q (linac, β=1)	190 Ω

Cavity Design and Fabrication

The cavity electro-magnetic design is based on a 1.6 cell all SC structure originally designed by Jacek Sekutowicz (DESY) with a lead cathode deposited on the half cell's backwall [4]. The cell shapes are optimized for maximum field on the cathode surface to allow a high launch field to minimize the beam's normalized emittance. Table 1 gives an overview of the figures of merit, Figure 1 shows the field distribution of the TM_{010} π-mode calculated by CST MWS™. The RF design was slightly changed in comparison to [4] to meet the 1.3 GHz and achieve the maximum electric field on the cathode surface. Further the mechanical passive stiffening was optimized by combination of electro-magnetic and mechanical ANSYS™ simulations [5] to reduce microphonics. This was of major importance as the cavity was foreseen without active tuning mechanism. Figure 2 shows the fully assembled gun cavity after fabrication, BCP and high pressure water cleaning, first vertical RF tests and installation of all ancillary components at JLab prior to shipping to A. Soltan institute for the cathode deposition. The manufacturing process is described in more detail in [6]. The 1.6 cells were made from polycrystalline RRR 300 niobium, whereas the halfcell's backwall was machined from large grain niobium with similar purity. After final tuning a field flatness of 94% was measured with a slightly lower field in the half cell.

* Work supported by Bundesministerium für Bildung und Forschung and Land Berlin
† Axel.Neumann@helmholtz-berlin.de

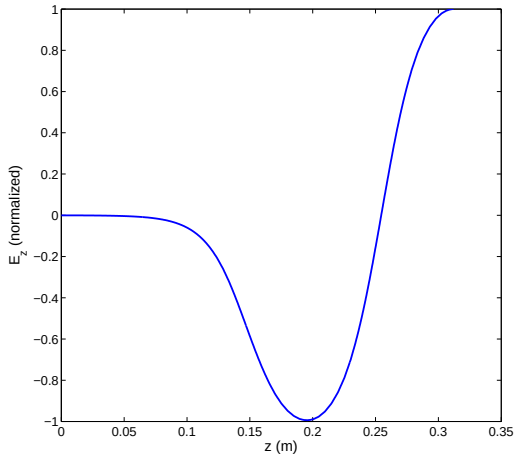

Figure 1: Normalized field amplitude E_z of the 1.6 cell SC gun cavity.

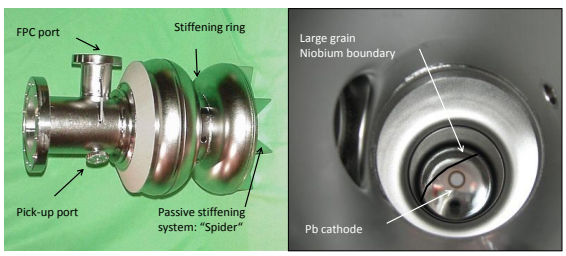

Figure 2: The picture on the left shows the 1.6 cell SC gun cavity after production and assembly of all ancillary components at JLab, the right picture shows the greyish lead cathode on the half cell backwall.

The cavity is equipped with a fundamental power coupler port for a TTF-III coupler allowing external Qs from about $1 \cdot 10^9$ down to $6 \cdot 10^6$. This permits the measurement of the intrinsic quality factor at a rather low coupling $\beta_c \approx 3...4$ while covering the CW beam operating range ($1 \cdot 10^7$ to $5 \cdot 10^6$) with microphonics. Further a standard TESLA field pick-up probe is installed as well as a stiffening ring and the passive stiffening system by 8 radial niobium bars on the backplate.

At the A. Soltan Institute the lead cathode was deposited on the large grain niobium back wall of the half cell by plasma arc deposition. After visual inspection of the lead spot as shown in the right picture of Figure 2, the cavity was sent to JLab again to remove the remnants of the lead deposition from the remaining niobium surface and to define the final cathode diameter by a final BCP and HPR treatment with a special protective mask for the cathode. The cathode has a final diameter of about 5 mm and an estimated thickness of 0.5 μm. After the final treatment the cavity was sent from JLab to HZB for installation in HoBiCaT and to install the warm diagnostic beamline.

Experimental Setup at HoBiCaT

Figure 3 displays the entire experimental setup. The gun cavity is installed in the HoBiCaT cryostat directly followed by a vacuum valve and the superconducting solenoid. The first vacuum port is for the pumping station to control the beamline and cavity vacuum. It is followed by the laser port for the UV λ=258 nm cathode laser developed by the Max-Born Institute. This port also has a moveable mirror unit to observe the steering of the laser on the cathode with a CCD camera. Next to the laser port is the first diagnostic port with a moveable YAG viewscreen or a Faraday cup. Further downstream there are a integrating current transformer and a stripline beam position monitor which have not been commissioned so far. At the end of the forward beamline is a viewport foreseen for THz spectroscopy to measure the bunch length and another viewscreen/Faraday cup setup. For beam spectroscopy we use a dipole magnet with a dispersive arm. This is also equipped with a viewscreen and a Faraday cup.

The cavity was operated with a phase-locked loop setup for the quality factor measurements with pulsed and CW RF methods at rather low β_c. For beam operation the cavity was driven via Cornell's LLRF system (see [8], [9]) at a bandwidth from 100-200 Hz with a 400 W solid state amplifier or a 17 kW IOT. To cope with the Lorentz-force detuning during ramping of the field to up to E_{peak}=20 MV/m and to compensate for slow drifts, the piezo tuning signal of the LLRF system was lowpass filtered to steer the master oscillator's frequency via a slow PLL frequency modulation. This same reference frequency was used to synchronize the laser system's internal PLL to the RF to allow fixed-phase particle acceleration.

During the measurements the laser was mainly operated at a repetition rate of 8 kHz but various pulse energies by changing the pump current of the laser amplifier. The used operating range of the solenoid was up to 100 mT.

FIRST HORIZONTAL RF MEASUREMENTS

After installation of the cavity and beamline in the HoBiCaT shelter the first horizontal RF test was performed to compare these with Q_0 measurements in the vertical test stand at JLab. Figure 4 summarizes the most important measurements. It depicts results before and after laser cleaning of the lead cathode with an excimer krypton-fluoride 248 nm laser.

The first vertical test of the fully assembled cavity (without cathode) achieved excellent results with $Q_0 \geq 1 \cdot 10^{10}$ at E_{peak} $\leq$35 MV/m with a field emission onset between 35-40 MV/m. The vertical test with the second cathode

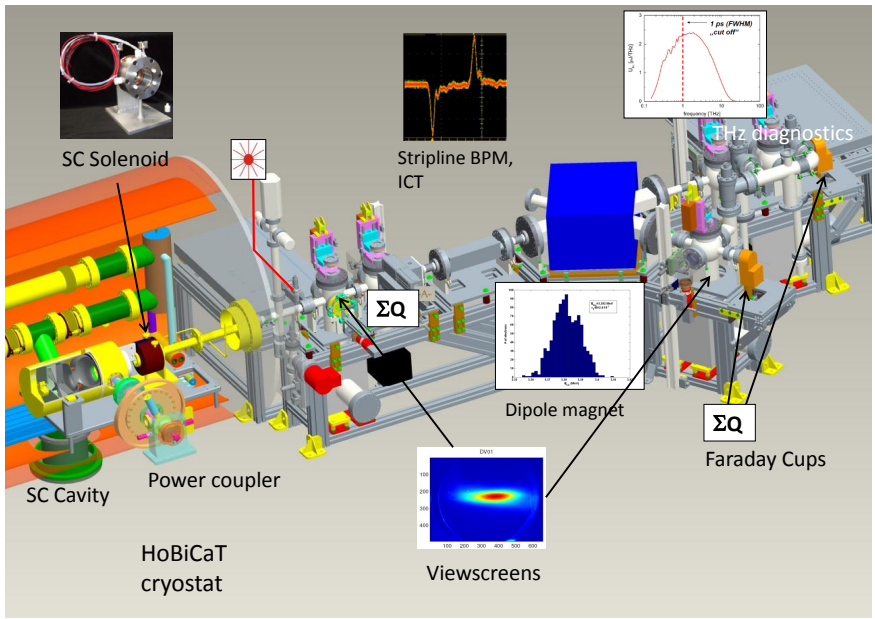

Figure 3: Overview of the measurement setup for the SC gun cavity tests at HZB including the HoBiCaT cryostat with the cavity and SC solenoid and the warm diagnostic beamline including viewscreen ports, Faraday cups, an ICT and stripline BPM as well as a dipole for energy measurements and the planned Terahertz diagnostics for the bunch length measurement.

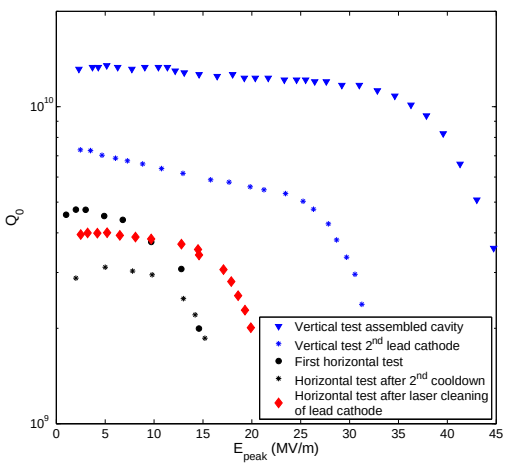

Figure 4: Measured unloaded quality factor versus peak electric field after cavity assembly and treatment in the vertical test stand (blue triangles) at JLab, after deposition of the second cathode (blue stars), the first horizontal test after installation and beam line assembly at HZB (black circles), after second cooldown at HZB (black stars) and after laser cleaning of the lead cathode(red diamonds).

deposited[1] showed already a degradation of Q_0 down to

[1]The first was accidentally lost during the vertical tests and BCP/HPR treatments

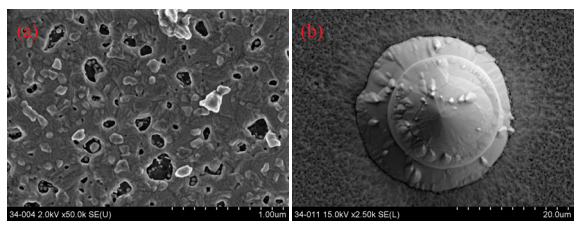

Figure 5: The pictures show SEM images (taken at FHI) of arc deposited lead samples by A. Soltan Institute similar to the gun cavity cathode. Small surface defects, droplets and tip on tip like structures in the 1-20 μm scale were observed.

$5 - 7 \cdot 10^9$ still allowing peak fields of 30 MV/m with an FE onset at 25 MV/m. The first horizontal measurement at a minimal $\beta_c \approx 3 - 4$ showed a further reduction of the Q_0 values down to $4 \cdot 10^9$ with field emission onset at 12 MV/m peak field. The low-field Q_0 was even lower after another cooldown cycle for some maintenances work, possibly the cold cavity collected all residual gas of the beamline during cooldown. After the laser cleaning of the cathode the surface resistance not only recovered to the initial horizontal value, but also the onset of field emission was shifted to a much higher level of 18 MV/m.

Laser cleaning resulted in a reduction of the dark current and radiation dose from the cathode, suggesting that some field emitters were removed. From this viewpoint laser cleaning of cavity niobium surfaces might be an in-

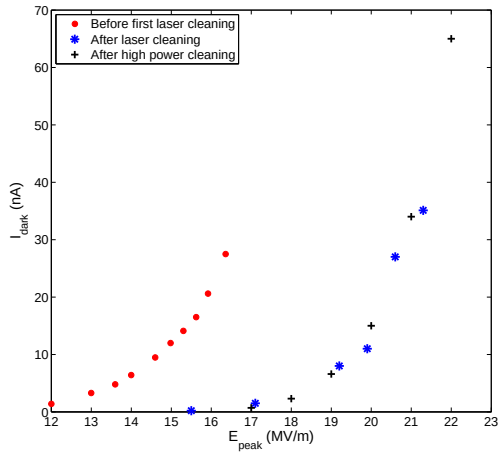

Figure 6: Measured dark current versus peak electric field by focussing the dark current with the SC solenoid on the first viewscreen before and after laser cleaning treatment of the cathode.

teresting option, something we will try in the future.

Figure 5 [10] shows a SEM image of arc deposited lead films on a multigrain niobium surface which were produced by the A. Soltan Institute in the same way as the lead cathode. Droplets and tip on a tip like structures [11] on the 1-20 μm scale were detected, possible candidates for strong field emitters.

Dark Current and Quantum Efficiency Studies

Any kind of dark current by strong field emitters may contribute to beam halo formation downstream in the accelerator beamline and thus be a major source for beam losses in the ERL's return arc. As it is crucial to minimize halo formation and beam loss, dark current characterization is a subject of these investigations.

Figure 6 shows an overview of the dark current measured with the first Faraday cup by focussing the beam on the corresponding viewscreen first. The three curves show the average dark current versus E_{peak} at different stages of the gun measurement program, including the laser cleaning. The laser cleaning seemed to shift the field emission onset from 12 MV/m up to 16-17 MV/m. In Figure 7 the Nordheim-Fowler equation [12, 13]

$$\bar{I}_F = \frac{5.7\times10^{-12}\times10^{4.52\Phi^{-0.5}}A_e(\beta E_0)^{2.5}}{\Phi^{1.75}} \times \exp\left(-\frac{6.53\times10^9\Phi^{1.5}}{\beta E_0}\right) \quad (1)$$

with $\bar{I}_F$ the average current emitted over one RF cycle, Φ the materials work function, A_e the emitters effective area, β the field enhancement factor and E_0 the surface electric field in V/m has been fitted to the measured dark current ($ln(\bar{I}E_0^{2.5})(1/E_0)$). Preliminary results show that after the laser cleaning the field enhancement factor was reduced

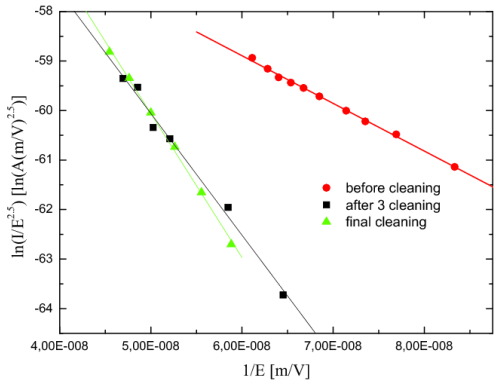

Figure 7: Fit of the Nordheim-Fowler field emission equation to the measured dark current values. The final cleaning was done with the highest power level throughout these measurements.

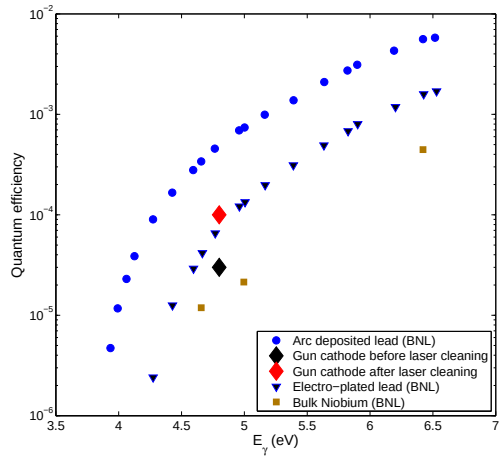

Figure 8: Comparison of measured quantum efficiency (QE) versus laser pulse energy at BNL [7] of electro-plated, arc-deposited lead and bulk Niobium samples with the QE obtained for the arc-deposited lead cathode of the 1.6 cell cavity before and after laser cleaning.

by a factor of three from 626 to 207 while the effective emitting surface increased by a factor of 1000. This may hint at sharp tips on the surface being smoothly leveled by the laser cleaning. It was also shown that already the first laser cleaning improved the dark current performance, the following cleaning with even higher laser power did not change its characteristics.

Figure 8 shows the measured quantum efficiency (QE) at 258 nm of the lead cathode before and after the laser cleaning. It was improved by a factor of three but is still below the best values achieved with arc deposited lead samples measured by [7]. A typical phase scan of the beam current at E_{peak}=18 MV/m versus the relative launch phase is displayed in Figure 9. This permits the extraction of QE and bunch pulse length information. At best beam currents of

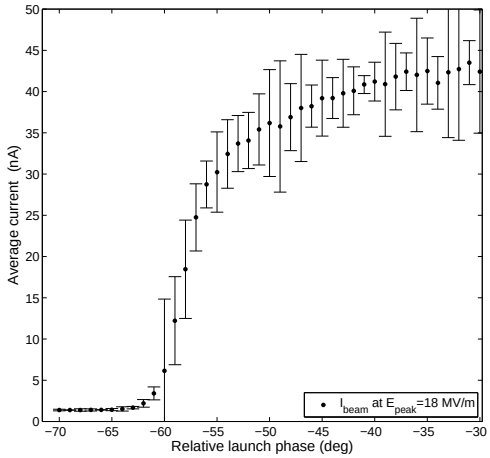

Figure 9: Phase scan of the emitted average beam current at E_{peak}=18 MV/m measured with the first Faraday cup at a laser repetition rate of 8 kHz.

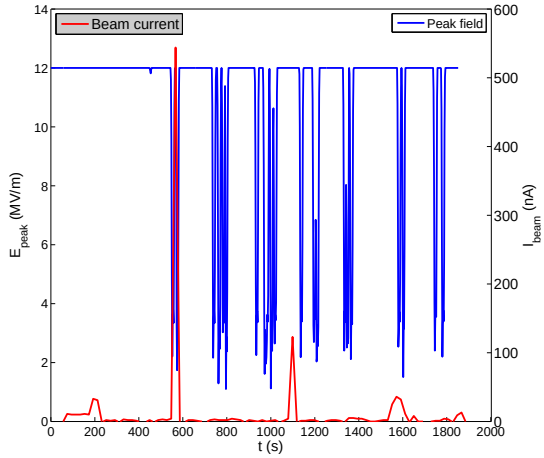

Figure 10: E_{peak} and average beam current versus time during the observation of cavity field trips at specific cathode positions. Sometimes currents above 500 nA were observed.

40 nA at 8 kHz laser repetition rate could be extracted with pulse lengths varying from σ=3-4 ps.

Intense studies of the QE and QE maps of the cathode in dependance of launch phase, laser power, laser spot size and launch field on the cathode were performed and will be presented in the near future in [14]. Further results with the cavity will be also presented in [15].

CAVITY FIELD TRIPS

During normal beam operation at different field levels frequent cavity field trips were observed when illuminating specific spots on the cathode with the drive laser. Simultaneously significant electronic activity was observed on the screens. It was shown, that these spots inhibited a stronger fluorescence in the visible range by observing the cathode with the CCD cathode camera (see Figure 12). Though the Faraday cup has a rather low bandwidth sometimes increased average beam currents of above 500 nA were measured just in coincidence with a field trip (Figure 10). Measuring the time constant of the transmitted power probe signal during such an event ruled out a cavity trip by a quench of the superconductor (Figure 11). Merely the strong beam current emitted in a short time interval extracts too much energy of the accelerating mode such that the LLRF system cannot supply enough RF power and the field trips within hundreds of ns. To understand this effect and to verify that this may be some kind of laser driven field emission the following measurement was done. The laser pulse energy was stepwise increased from the lowest possible energy where still some current above the resolution limit of the Faraday cup (1 nA limited by readout) could be detected. It was shown that below a certain threshold pulse energy no trip occurred. Furthermore, above that level the time after which a trip occurred depended on the laser

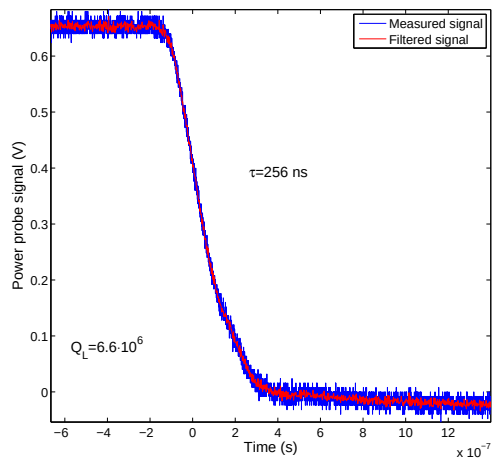

Figure 11: Transmitted power probe signal versus time during a cavity field trip event. The time constant of 256 ns rules out any cavity quench triggered trip.

power level (constant rep. rate). Also the beam current was at a level as expected from the QE at these spots, only during the trip the beam current increased to several hundred nanoamperes. Interestingly, the such processed cathode spot showed less fluorescence after this measurement as can be seen in Figure 12 without a significant change of the QE. This will be further analyzed in the future.

FIELD STABILITY AND BEAM ENERGY

Bunch-to-bunch energy and time jitter of the beam produced by the gun also depends on the field stability of the CW operated cavity. Figure 13 shows a typical microphonics detuning spectrum taken at a peak field level of 20

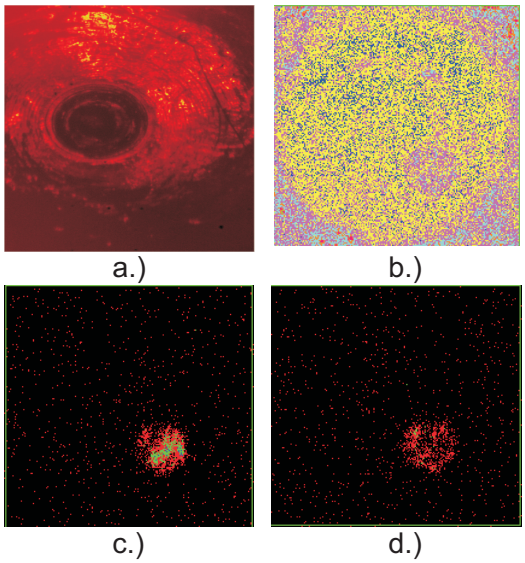

Figure 12: a.) False color picture of the halfcell backwall with the whole cathode visible as a black spot. b.) Laser spot located on a cathode region where cavity trips occur at any extraction phase (magenta spot on yellow surface). c.) Optical photo of the UV cathode laser illuminating the cathode, strong fluorescence can be observed. d.) After several measurements with different laser power on that same cathode location the fluorescence seems reduced. b.)-d.) only show the cathode area.

MV/m with the LLRF's ring buffer. Besides strong excitations at about 47 and 70 Hz, where the source is unknown so far, a mechanical eigenmode at 252 Hz was detected. Long term measurements over more than six hours showed an rms detuning between 5-7 Hz and a peak detuning of 25 Hz. As this cavity was not equipped with a tuner, the only way to extract information about the coupled system of the electro-magnetic field and the mechanical system of the cavity cells is to measure the transfer function using dynamic Lorentz-force detuning [16].

The transfer function between the amplitude modulated forward power and the cavity detuning is given in Figure 14. Up to 200 Hz the response is flat, at 250 Hz a group of four mechanical eigenmodes is excited by the sinusoidal varying field amplitude in the cavity.

The cavity was operated at peak field levels between 10 and 20 MV/m ($E_{acc} = 5.5 - 11$ MV/m) at loaded quality factors of $1.4{\cdot}10^7$ down to $6.6{\cdot}10^6$. Table 2 summarizes the measured rms microphonics detuning, the rms phase and relative amplitude stability routinely achieved with the Cornell LLRF system assisted by the slow sub-hertz PLL frequency correction. The rms detuning seems to be slightly increased at a higher field level, but probably this is mainly due to the increased cavity-loop system bandwidth at the lower Q_L. Additionally the pressure sensitivity of the cavity was determined as 114 Hz/mbar, validating the measured value in the vertical test stand of about 100 Hz/mbar [6].

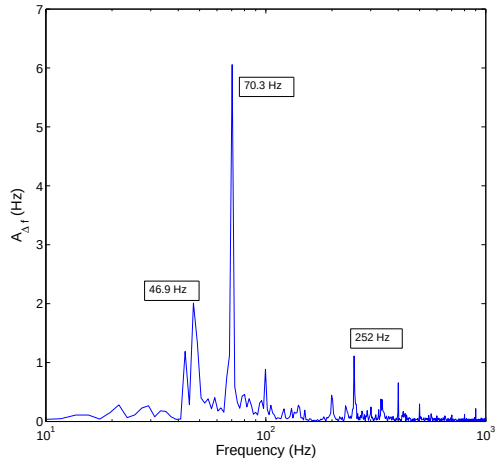

Figure 13: Microphonics detuning spectrum of the gun cavity in CW operation at $Q_L = 6.6 \cdot 10^6$. The line at 252 Hz is an excited mechanical resonance which was measured by dynamic lorentz force detuning excitation.

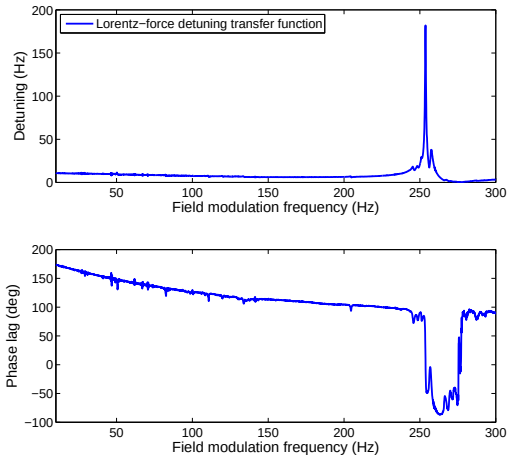

Figure 14: Dynamic Lorentz-force detuning transfer function in detuning amplitude versus forward power modulation frequency (upper plot) and phase response. A group of four strong mechanical eigenmodes was found at around 250 Hz.

Beam Energy

The beam's kinetic energy was measured by the dispersive section of the beam line using the dipole current and the Faraday cup signal maximized crosschecked with the YAG viewscreen to determine the position of the maximum of the beam distribution. Figure 15 displays two scans of the beam energy over launch phase at 12 and 20 MV/m field at the cathode. To understand the longitudinal beam dynamics, especially to learn how to improve the RF de-

Table 2: Cavity field stability

Q_L	E_{peak} (MV/m)	σ_f (Hz)	σ_Φ (deg)	σ_A/A
$1.4 \cdot 10^7$	12.0	5.02	0.02	$1.5 \cdot 10^{-4}$
$6.6 \cdot 10^6$	20.0	7.0	0.017	$1.2 \cdot 10^{-4}$

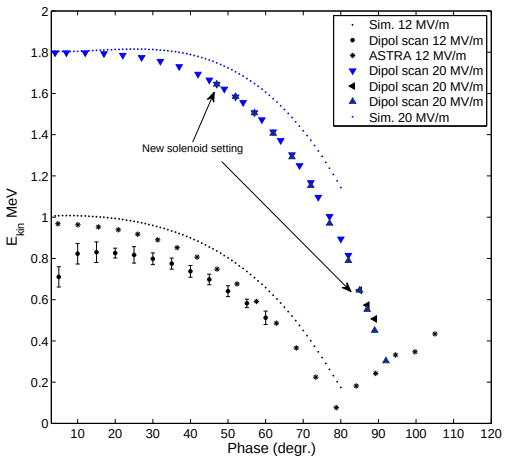

Figure 15: Measured beam kinetic energies for 12 and 20 MV/m launch field versus phase compared to ASTRA and longitudinal tracking simulations.

sign for the future B*ERL*inPro gun cavity, the result was reconstructed with a self written longitudinal tracking code and ASTRA [17] simulations. It was not fully possible to reconstruct the curvature of the measurement which did not show the small local maximum at a phase of about 30 degrees for 20 MV/m, even when taking into account the imperfect field flatness. For the next measurements a careful calibration of the dipole and the cavity field is foreseen.

OUTLOOK

First measurements of the beam's normalized emittance and the thermal emittance of the lead cathode have been started, as well as studies of bunch length in the presence of space charge effects. These measurements will be further pursued late summer this year and first results will be published in [14]. Recently the cryostat was warmed up again to improve the diagnostics capabilities of the beamline and the alignment of the cavity to the solenoid. This will allow a more accurate measurement of the emittance and to start studies about the beam energy spread and jitter. Further the cavity trip events will be studied in more detail.

Lessons learned with this cavity will be incorporated in the RF design of the future B*ERL*inPro injector cavity, optimizing the cavity shape for higher launch phases.

REFERENCES

[1] M. Abo-Bakr *et al.*, "B*ERL*inPro- An Accelerator Demonstration Facility for ERL-based Light Sources", Proc. of the 25th LINAC (2010), Tsukuba, Japan, http://www.JACoW.org.

[2] T. Kamps *et al.*, "SRF Gun Development for an Energy-Recovery Linac based Future Light Source", Proc. of the 14thSRF Conference (2009), Berlin, Germany, http://www.JACoW.org.

[3] T. Kamps *et al.*, "Status and perspective of superconducting radio-frequency gun development for B*ERL*inPro", Journal of Physics: Conference Series, **298** (2011), http://iopscience.iop.org/1742-6596.

[4] J. Sekutowicz, A. Muhs, P. Kneisel, R. Nietubyc, "Cryogenic Test of the Nb-Pb SRF Photoinjector Cavities", Proc. of the 23rd PAC (2009), Vancouver, Canada, http://www.JACoW.org.

[5] A. Neumann *et al.*, "CW Superconducting RF Photoinjector Development for Energy Recovery Linacs", Proc. of the 25th LINAC (2010), Tsukuba, Japan, http://www.JACoW.org.

[6] P. Kneisel *et al.*, "Fabrication, Treatment and Testing of a 1.6 Cell Photo-injector Cavity for HZB", Proc. of the 24th PAC (2011), New York, USA, http://www.JACoW.org.

[7] J. Smedley *et al.*, "Lead photocathodes", PRST-AB, Volume 11, No. **1**, 2008, DOI: 10.1103/PhysRevSTAB.11.013502.

[8] M. Liepe *et al.*, "Experience with the New Digital RF Control System at the CESR Storage Ring", Proc. of the 21st PAC (2005), Knoxville, USA, http://www.JACoW.org.

[9] A. Neumann *et al.*, "CW Measurements of Cornell LLRF System at HoBiCaT", these proceedings.

[10] R. Barday *et al.*, "Instrumentation needs and solutions for the development of an SRF photoelectron injector at the Energy-Reocvery Linac B*ERL*inPro", Proc. of the 10th DIPAC (2011), Hamburg, Germany, http://www.JACoW.org.

[11] H. Padamsee, J. Knobloch, T. Hays, "RF Superconductivity for Accelerators", Wiley-VCH, Second Edition, Weinheim, Germany, 2008.

[12] R.H. Fowler, L. Nordheim, "Electron Emission in Intense Electric Fields", Proc. R. Soc. Lond. A May 1, 1928 119:146-156;

[13] J.H. Han *et al.*, "Dark current measurements at the PITZ RF Gun", Proc. of the 6th DIPAC (2003), Mainz, Germany, http://www.JACoW.org.

[14] T. Kamps *et al.*, "Demonstrating electron beam generation and characterization with an all superconducting radio-frequency photoelectron source ", Proc. of the 2nd IPAC (2011), San Sebastián, Spain (to be published).

[15] A. Neumann *et al.*, "First characterization of a fully superconducting RF photoinjector cavity", Proc. of the 2nd IPAC (2011), San Sebastián, Spain (to be published).

[16] A. Neumann, "Compensating microphonics in SRF Cavities to ensure beam stability for future Free-Electron-Lasers",Phd thesis, Humboldt Universität Berlin, Germany, 2008.

[17] K. Flöttmann, A Space Charge Tracking Algorithm (ASTRA), http://www.desy.de/∼mpyflo/.